Infectious Disease Modelling 8 (2023) 855–864

Contents lists available at ScienceDirect

Infectious Disease Modelling

journal homepage: www.keaipublishing.com/idm

An immuno-epidemiological model for transient immune protection: A case study for viral respiratory infections

A. Hoyer-Leitzel [a, *], S.M. Iams [b], A.J. Haslam-Hyde [c], M.L. Zeeman [d], N.H. Fefferman [e]

[a] Department of Mathematics and Statistics, Mount Holyoke College, 50 College St, South Hadley, MA, 01075, USA
[b] John A. Paulson School of Engineering and Applied Sciences, Harvard University, USA
[c] Department of Mathematics and Statistics, Boston University, USA
[d] Department of Mathematics, Bowdoin College, USA
[e] Dept of Mathematics & Dept of Ecology and Evolutionary Biology & NIMBioS, University of Tennessee, Knoxville, USA

ARTICLE INFO

Article history:
Received 29 December 2022
Received in revised form 14 June 2023
Accepted 8 July 2023
Available online 16 July 2023
Handling Editor: Dr Yijun Lou

Keywords:
Flow-kick dynamics
Immuno-epidemiology
Viral-immune mathematical model
Immune boosting
Priming number

ABSTRACT

The dynamics of infectious disease in a population critically involves both within-host pathogen replication and between host pathogen transmission. While modeling efforts have recently explored how within-host dynamics contribute to shaping population transmission, fewer have explored how ongoing circulation of an epidemic infectious disease can impact within-host immunological dynamics. We present a simple, influenza-inspired model that explores the potential for re-exposure during a single, ongoing outbreak to shape individual immune response and epidemiological potential in non-trivial ways. We show how even a simplified system can exhibit complex ongoing dynamics and sensitive thresholds in behavior. We also find epidemiological stochasticity likely plays a critical role in reinfection or in the maintenance of individual immunological protection over time.

1. Introduction

For the majority of their development and analysis, epidemiological models have treated the process of replication of a pathogen within individuals as a black-box (Anderson & May 1992). The fundamental insight of epidemiological models is that outbreaks are emergent properties of populations. They result from individual transmission and infection dynamics (Anderson & May 1992; Brauer et al., 2008; Castillo-Chavez et al., 2002; Keeling & Rohani, 2011). In this context, treating replication as a black box is a reasonable simplification and has allowed for profoundly beautiful and important insights into the dynamics of outbreaks (Lofgren et al., 2014). However, recent work has begun to pay more attention to the explicit role of the individual within these epidemiological processes: behavioral models have looked at contact networks (Hock & Fefferman, 2012; Keeling & TD Eames, 2005; Silk & Fefferman, 2021); pathogen models have considered heterogeneity in individual rates of viral shedding that could lead to “superspreaders” (Allen et al., 2012; Lloyd-Smith et al., 2005); and

* Corresponding author.
E-mail address: ahoyerle@mtholyoke.edu (A. Hoyer-Leitzel).
Peer review under responsibility of KeAi Communications Co., Ltd.

https://doi.org/10.1016/j.idm.2023.07.004

immuno-epidemiological models have considered the coupled dynamics of within-host replication and among-host transmission (to understand temporal patterns (Kostova, 2007) or to consider strain competition for pathogens where there may be trade-offs in fitness (Saad-Roy et al., 2022)). These models have greatly enhanced our epidemiological understanding. However, they have not provided a complete understanding of the interplay between individually infected hosts and population-wide outbreaks. Such outbreaks emerge from the interactions of infected hosts and their community. In this paper, we will focus on within-host dynamics of short-term immune function under conditions of frequent re-exposure that might be expected during the circulation of a pathogen during an outbreak.

The study of drivers of ongoing transmission of infection during an outbreak focuses on characterizing the role of identifiably unwell individuals (Cope et al., 2018; Hart et al., 2019; Kretzschmar & Wallinga, 2009). However, sources of infection can be hard to identify. Infectious people can shed pathogen into their environment to be picked up later (e.g., fomite or aerosol transmission) (NM Kraay et al., 2018). Some diseases can cause active infection without symptoms (asymptomatic cases), meaning that identification of sources of infection is not always possible (Saad-Roy et al., 2020). For some diseases, some asymptomatic shedders may be carriers (e.g. Gunn et al., 2014). Carriers, unlike typical asymptomatic infection-shedding hosts, do not clear the infection. Instead, they remain in a long-term state of active, albeit sometimes low-level, infection (e.g. Villa et al., 2011). Infection processes also depend critically on the pathogen exposure dose (Brooke et al., 2013; Buchanan et al., 2000). Some pathogens can successfully infect a susceptible host with only a few viri or microbes (Teunis et al., 2008), where others require exposure to massive doses of infection to transmit (Gale, 2001, 2005). This complexity is the result of interactions between pathogen biology and host immune function (Maul, 2014).

Human immune function is the combination of a diverse and complicated set of physiological responses to external stimuli (Brodin & Davis, 2017; Peter Parham, 2014). The most rapid responsive component of immune function is the innate immune system (Beutler, 2004), with adaptive immunity ramping up more slowly, allowing a more specific and durable response (Bonilla & Oettgen, 2010). This is observable as short bursts of broad innate protection, yielding its function to longer, targeted (and potentially multifaceted) protection (Bonilla & Oettgen, 2010). As a result, for a particular host and pathogen, the timing of viral exposure relative to the state of immune function may affect the potential for that exposure to cause infection.

When considering the dynamics within a single outbreak of an infectious disease in a population under traditional epidemiological modeling assumptions, uninfected hosts are either susceptible to infection from exposure to an infective individual (the “S” compartment), or not (the “R” compartment) (Anderson & May 1992). However, as we have just discussed, individual susceptibility relies on a variety of interacting, ongoing processes. This means that re-exposure of previously infected people may play a critical boosting role in the maintenance of immune protection. While this has been studied in longer-term dynamics of adaptive immunity over multiple outbreaks (Lavine et al., 2013), we will focus our attention on the short-term interplay of re-exposure during a single, initial epidemic.

One potentially interesting short-term impact of re-exposure is that recovered individuals might hover in an epidemiological gray zone. In this state they are protected from becoming newly symptomatic from sequential exposures themselves, but may still be able to replicate pathogen for a few days of subclinical or asymptomatic infection, which may be enough to continue spreading low-dose exposure to others. This has the intriguing possibility of propagating ongoing protection to immune or partially immune individuals without requiring true reinfection of those individuals. This is the equivalent of a natural, transmissible booster shot. Of course, if a susceptible individual is exposed to a sufficient number of low-dose shedders within a short time period, this may be the cumulative equivalent of one high-dose exposure to an active, symptomatic infection in ways that might never be differentiable by observation.

The outcome of individual re-exposure to a pathogen during an outbreak may critically rely on current population-level prevalence of both active infection and subclinical early-stage infections that will never blossom into full replication due to effective immune containment. The frequency of cases that “tip over” into active, replicating, clinical infection constitutes the observable outbreak. This transition to active infection may be due to heterogeneity of immune function or due to cumulative stochastic exposure exceeding some critical individual threshold. Ongoing epidemics would be the result of both subclinical re-exposure and larger dose exposure from actively, symptomatically infected individuals. This complexity cannot be fully understood by tracking case counts.

This more nuanced epidemiological reality calls for more nuanced mathematical modeling. Where standard compartmental models and systems of ordinary differential equations are excellent for examining population level epidemic processes, flow-kick systems are appropriate for extending these models to explore the potential impact of regular re-exposure of infection. In a flow-kick model, periods of continuous flow, such as immune system response to an exposure event (modeled by a differential equation), repeatedly alternate with discrete kicks, such as re-exposure events (modeled by discrete increases in pathogen). Previous studies of flow-kick dynamics have provided insight into fishery systems subject to regular harvesting events (Zeeman et al., 2018; Meyer et al., 2018), eutrophication in lakes subject to pulses of nutrients (Meyer et al., 2018), coral reefs subject to hurricane damage (Stephen et al., 2016), tick spread in an ecosystem subject to fire (Alexander et al., 2022), neurobiology of drug addiction (Chou & D'Orsogna, 2022), and savanna systems subject to regular fire events (Hoyer-Leitzel & Iams, 2021; Tamen et al., 2016, 2017).

Using a flow-kick model, we study how transmissible “boosting” exposure and how the relative frequency of exposure at various magnitudes (whether from active infection or from immune-contained reinfection) may affect individuals in populations during an ongoing epidemic outbreak. We build on a published model of immune function (Cao et al., 2015), designed and parameterized with influenza infection in mind. We do not mean for these first investigations to be understood as an accurate model of influenza dynamics. Instead, we use this formulation and parameterization to provide proof of

concept in a single case study. The functional forms and parameter set we assume in our system of equations are reasonable but are not actually known in most cases. The exact choices are likely to significantly impact the studied behaviors of our system. In addition, the model on which we build is itself a specialized choice, focusing on the local availability of invasible tissue for pathogen to infect (e.g., lung tissue targeted by respiratory infections), and therefore would be inappropriate for pathogens that are not tissue-limited. We leave it to future work to investigate the sensitivity of our particular results to these choices. Instead, we present this model and our current results to highlight the importance of these types of dynamics in understanding epidemics, and to invite additional attention to the study of such systems.

2. Methods

Within-host immune system model: To simulate within-host immune response to an influenza-like respiratory virus, we use a modification of the model proposed by Cao et al. (Cao et al., 2015). The model, conceptually depicted in Fig. 1, consists of six ordinary differential equations which account for the dynamics of virus (V), target cells (T), infected cells (I), interferon (F), B-cells (B), and antibodies (A). In the model, interferon kills infected cells and antibodies (produced by B-cells in the presence of virus) inhibit virus. This model arises by setting $\varphi = \rho = \xi = s = 0$ in (Cao et al., 2015), to effectively remove virus-resistant cells from their model ($R = 0$). Of note, there is an infection-free equilibrium when the target cells are at capacity ($T = C_T$), and all other variables are zero.

We have also modified the virus-target cell interactions by introducing a unitless switching function ($V/(V_m + V)$), which is zero when $V = 0$, 1/2 when $V = V_m$ and approaches 1 as V increases. The result is that the virus-target cell interaction is primarily the same as in (Cao et al., 2015), but the interaction turns off as the number of virions falls below a threshold, as in (Pascucci & Pugliese, 2021). The modification by this term stabilizes the infection-free equilibrium for very small levels of virus ($V < V_m$). This reflects a realistic dose-response behavior, which is well-approximated by continuous dynamics under sufficient viral presence, but for which tiny discrete (or even fractional) numbers of viri cannot cause cascading replication leading to active infection. The model is given by Equation (1). The parameters are specified in Table 1.

$$\begin{aligned}
\dot{V} &= pI - cV - \mu VA - \beta VT\frac{V}{V_m + V}\\
\dot{T} &= gT\left(1 - \frac{T+I}{C_T}\right) - \beta' VT\frac{V}{V_m + V}\\
\dot{I} &= \beta' VT\frac{V}{V_m + V} - \delta I - \kappa IF\\
\dot{F} &= qI - dF\\
\dot{B} &= m_1 V(1 - B) - m_2 B\\
\dot{A} &= m_3 B - rA - \mu' VA
\end{aligned} \tag{1}$$

Viral exposures: We model a sequence of viral exposures of size k_n at times t_n ($n = 1, 2, 3, \ldots, N \leq \infty$) by impulses making instantaneous changes to V. Thus

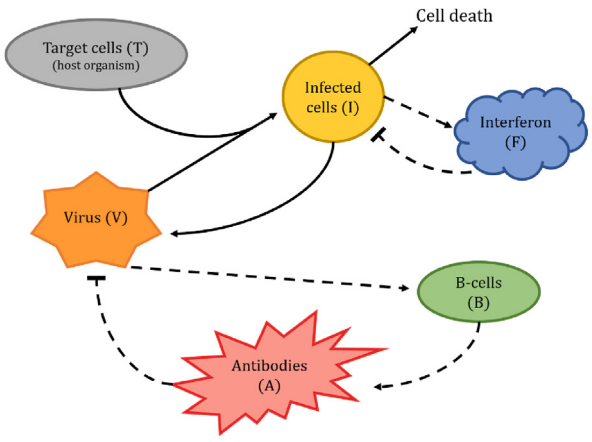

Fig. 1. The virus (V), target cells (T), and infected cells (I) constitute a three-variable subsystem wherein virus infects target cells to produce infected cells and infected cells produce more virus. The innate immune function is represented by interferon (F) which is produced in the presence of infected cells and inhibits viral production by killing infected cells. Adaptive immunity in the model consists of B-cell (B) activation in the presence of virus, antibody (A) production in the presence of B-cells, and neutralization of viri by antibody.

Table 1
Default parameter values for the model. Units of V, F, and A are denoted u_V (number of viri), u_F and u_A respectively. T and I have the same units, u_T (number of cells). B is a unitless number between 0 and 1. Time is measured in units of days (d). All parameter values are from (Cao et al., 2015), with the exception of V_m and k. The threshold, V_m, is set to 10 viri, and is orders of magnitude smaller than k.

Par	Description	value	units
P	viral production rate	0.35	$u_V/(u_T d)$
C	viral clearance rate	20	$1/d$
M	rate of viral loss per unit of antibodies	0.2	$1/(u_A d)$
μ'	rate of antibody loss per virion	0.04	$1/(u_V d)$
B	rate of viral loss per target cell	5×10^{-7}	$1/(u_T d)$
β'	rate of conversion from target cells to infected cells per virion	2×10^{-5}	$1/(u_V d)$
V_m	half-activation for viral growth	10	u_V
G	basal growth rate of healthy target cells	0.8	$1/d$
C_T	maximum cell capacity of the target tissue	7×10^7	u_T
δ	death/removal rate of infected cells	3	$1/d$
κ	killing rate of infected cells per unit of interferon	3	$1/(u_F d)$
q	interferon production rate	1×10^{-7}	$u_F/(u_T d)$
d	interferon degradation rate	2	$1/d$
m_1	rate of B-cell activation per virion	1×10^{-4}	$1/(u_V d)$
m_2	rate of B-cell deactivation	0.01	$1/d$
m_3	antibody production rate from B-cells	12000	u_A/d
r	antibody degradation rate	0.2	$1/d$
k	kick size representing viral exposure	order 10^4	u_V

$$V(t_n^+) = V(t_n^-) + k_n \tag{2}$$

where $V(t_n^-)$ and $V(t_n^+)$ represent the value of V immediately before and after the kick at time t_n, respectively.

Define $\tau_n = t_n - t_{n-1}$ to be the flow-time between kicks k_{n-1} and k_n. We call the sequence $\{(\tau_n, k_n), n = 1, \ldots, N\}$ the *disturbance regime*, and (τ, k)-space the *disturbance space*. We call the disturbance regime *deterministic* or *periodic* if $(\tau_n, k_n) = (\tau, k)$ for all $n = 1, \ldots, N$, and *stochastic* if (τ_n, k_n) are drawn randomly from a probability distribution.

The response of the host to the sequence of viral exposures is given by the flow (or solutions) of Equation (1) after each kick. We simulate this in Matlab using `ode15s` to numerically solve Equation (1) between the kicks. To simulate the viral exposure events, at each kick time t_n we increase the viral state by the kick size k_n. Then we continue to solve Equation (1), with the new viral state, until the next kick time t_{n+1}.

See (Zeeman et al., 2018; Meyer et al., 2018) for alternative formulations of flow-kick models based on the time-τ_n maps of Equation (1). For this paper, we prefer the impulsive differential equation formulation, as our focus is on the transient behavior of the V excursions in the immune response between the kicks, which is too fast to be captured by the time-τ_n maps for realistic re-exposure time intervals τ_n. Note that consequences of these excursions can be captured by the time-τ_n map in the slower variables, A and B.

Single exposure simulations: We are interested in identifying viral exposure sizes, k, applied to the infection-free equilibrium at time $t = 0$, that cause excursions corresponding to symptomatic infections. Since there are no infected cells at the time of exposure ($I = 0$), V will initially decrease immediately after exposure, as $\dot{V} < 0$ in Equation (1). An excursion is defined as a subsequent increase in the amount of virus to an amount bigger than the size of a kick during the flow period and can be thought of as detectable illness in the host. We use a bisection method to determine, to within 1 virion, the maximum size of viral exposure that does not produce an excursion.

Second exposure simulations: We use a similar method to find the maximum size of a second exposure that avoids an excursion, with the timing, $t = \tau$, of the second exposure set to values $5 \leq \tau \leq 400$. See Fig. 3. Here, an excursion is defined as an increase in V to an amount greater than immediately after the kick ($V > V(\tau^+)$) during the flow period. Each initial viral exposure is set to $V = 4000$ at time $t = 0$, and the size of the second exposure is also initially set to $V = 4000$. This second value is doubled until it triggers an excursion, at which point a bisection method is applied to identify the maximum second exposure value that avoids an excursion.

Repeated exposure simulations: To model periodic or stochastic re-exposure to virus, we use deterministic or stochastic disturbance regimes, respectively. We solve the flow-kick system for a total time of at least 400 days to identify long term behaviors. In the deterministic case, when looking for excursion thresholds in the flow-kick system, as in Fig. 5, we first set the periodic kick size at $k = 4000$, and then double this value until it triggers an excursion within 1500 days. Then a bisection method is applied to identify an approximation of the boundary of the blue protection region in Fig. 5. We use a lattice with $\Delta\tau = 0.1$ and $\Delta k = 1$ along a linear approximation of the boundary and check each point in the lattice for an excursion within 1500 days.

Parameter Sensitivity: We analyzed this system for parameter values given in Table 1. To look at parameter sensitivity, we examined the impact of an increase or decrease of 10% in each parameter. The parameter set in Table 1 lies near a subcritical Hopf bifurcation of one fixed point in the underlying system. For most of the parameters, it is possible to cross the Hopf bifurcation with a 10% change in value. However, the Hopf bifurcation is local to that specific fixed point, and that fixed point is

not close to the dynamics we are studying. Adjusting the parameters by 10% creates changes that are not visually detectable for the results in Fig. 2. It also does not have an effect on the boundary in Fig. 3.

Matlab scripts for the computations used for Figs. 2–5 are available at https://github.com/ahoyerleitzel/flow-kick-immune-system.

3. Results

Single exposure: In Fig. 2, we illustrate the model system state for 10 days following an initial exposure to infection. After exposure, there is a post-infection phase in which virus invades target cells and replicates in them, with innate interferon responses and B-cells also increasing. Adaptive antibodies increase over a longer time frame (with meaningful presence 3 days post exposure). The interferon response decreases rapidly after the number of infected cells is controlled, and B-cell numbers decrease gradually over time. Initial virus exposures of $k \geq 10$ give results quantitatively similar to those shown in Fig. 2.

Second exposure: Following the first exposure to infection, the modeled immune response is temporarily protective against infection from re-exposure to the same pathogen (see Fig. 3). For a moderate time period (50 days), the host remains robust against even massive doses of virus (an order of magnitude higher than the initial dose). That protection wanes over time. Lower and lower dose exposures are sufficient to cause some infection as time progresses. Nearly all protection is lost by approximately a year post initial infection so that a small dose of virus, just sufficient to cause infection in a naive host, will again lead to active infection in the previously-recovered host. This qualitatively mirrors expected biological dynamics, though the timing and magnitude are different for different hosts and pathogens (e.g. (Glass & Grenfell, 2004),).

Periodic repeated exposures: Using the same model, we explore periodic re-exposure following an initial infection, in which the host is re-exposed to the same viral dose (kick k) every τ days. This leads to two separate cases (see Fig. 4): one where periodic re-exposures protect against reinfection indefinitely, and one where the protection wanes over time and reinfection does occur.

In the first case (Fig. 4, A-F), periodic re-exposure causes immune function to remain protective against reinfection: there is never a large replication spike in virus after recovery from initial infection. Mathematically, the flow-kick system reaches equilibrium. In this case, the regular viral exposure is sufficient to keep immune function up-regulated, and insufficient to overwhelm the protection afforded by that primed immune response. As we saw earlier, this is not solely a function of the magnitude of the re-exposure dose, but also of the time between doses. Small viral doses that are introduced so quickly that they function as a single, cumulatively large dose may be able to overwhelm immune protection in ways that would not be possible with more time between exposure doses. Conversely, if the inter-exposure interval is too large (e.g., over a year in our initial example), protection is likely to have waned sufficiently so that each next exposure triggers a novel infection.

One intriguing possibility that is highlighted by this case is that medically detectable signals of protective immune up-regulation may be much subtler than currently expected, while still offering substantive protection. Neither antibody levels nor systemic inflammatory responses may seem meaningfully elevated, yet they would still provide just enough protective benefit, not to prevent all viral replication, but to sufficiently anticipate dose introduction and overwhelm viral replication with only modest responses. This means that there is the potential for meaningful protection, even when no infection or immune response would ever be noticed without a specific, targeted study looking for very subtle changes.

In the second case (Fig. 4, G-L), periodic re-exposure slightly prolongs the initial protection against reinfection, but over time the protection wanes, despite the periodic priming, and reinfection occurs. This case merits further analytical consideration than we present in this first exploration. It is intriguing that the re-exposures do slightly prolong the initial protection,

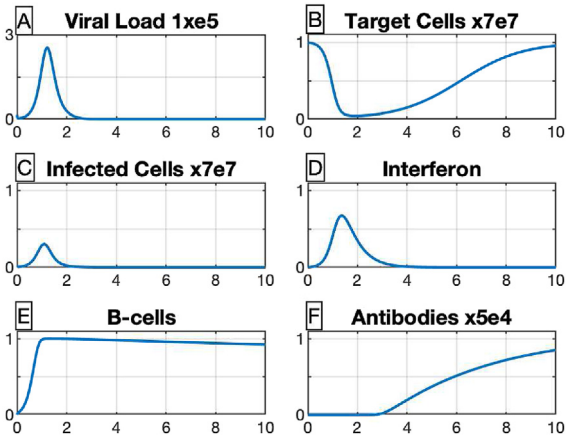

Fig. 2. Short term (10 day) immune response to a single viral exposure. **(A)**–**(F)** Baseline solution to the continuous system given in Equation (1) with an initial condition of $V = 15000$, $T = C_T$, and all other variables equal to 0.

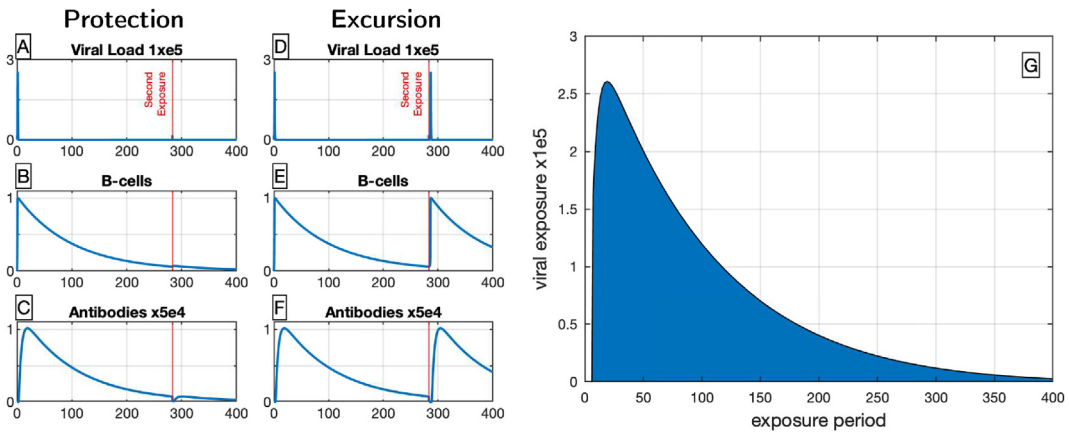

Fig. 3. **(A)**–**(F)** Long term (400 day) immune response with a second viral exposure at $\tau = 283$. **(A)**–**(C)** The viral dose is set to $k = 14800$, and there is no excursion after the second exposure. This corresponds a point in the blue region of (G). **(D)**–**(F)** The viral dose is set to $k = 15000$. This is the smallest (integer valued) second dose that triggers a second excursion at $\tau = 283$. This corresponds a point outside of the blue region of (G). **(G)** The viral re-exposure dose needed to trigger a second excursion depends on the timing of re-exposure. The shaded region shows the kick sizes (doses) that do not trigger a second excursion for each re-exposure time τ ($5 \leq \tau \leq 400$).

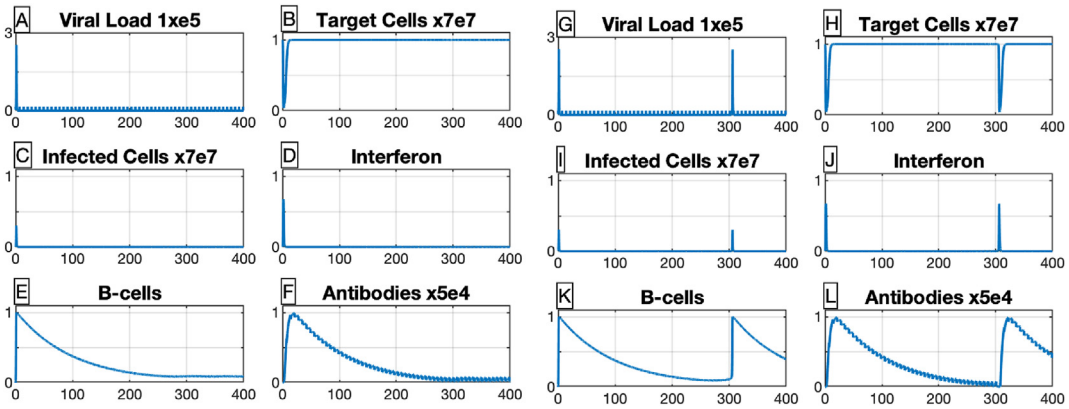

Fig. 4. Long term (400 day) immune response with viral re-exposure every 7 days. **(A)**–**(F)** Case 1: iteration of the flow-kick system with $(\tau, k) = (7, 15000)$. This combination of parameters (τ, k) leads to a stable flow-kick equilibrium corresponding to a protected state in which no reinfection occurs. For a finer time-scale depiction of this equilibrium, see Supplementary Figure A1 A-F. **(G)**–**(L)** Case 2: iteration of the flow-kick system with $(\tau, k) = (7, 16244)$, representing a state in which reinfection does occur. This is the smallest integer kick size that yields a second excursion when applied every 7 days. To see a finer time-scale depiction of the dynamics near the second excursion, see Supplementary Figure A1 G-L.

making it unclear how to predict when a new round of active infection will be triggered by a re-exposure. We will explore this phenomenon more fully in future work and hope others will join us in helping to understand the nuances of this system.

The dichotomy between periodic re-exposure patterns that do or do not provide long-term protection against reinfection is numerically plotted in Fig. 5. The blue area corresponds to re-exposure patterns that provide long-term protection. At the boundary, there is surprising periodicity in the re-exposure frequencies and magnitudes that provide protection against successive illness. The presence of periodicity means that differences in outcome that may be perceived as stochasticity and heterogeneity in host response to re-exposure could instead be aspects of the deterministic system. This highly structured excursion boundary reflects canard-like behavior that is associated with the periodic protection regions. This canard-like behavior separates regions of (τ, k) space in which there is only protection against reinfection until the N kick vs the $N + 1$ kick. See Supplemental Figure A2 to see part of (τ, k)-space where reinfection occurs colored by the number of kicks, N, after which there is reinfection.

The locations in (τ, k)-disturbance space of canard-like behavior may be set by slight differences in the coherence between viral dose and the immune state of the host in the flow dynamics of the recovery following illness. The precise dynamics and possible bifurcations that lead to this observed behavior merit further exploration, planned in our own future work.

Stochastic repeated exposures: One of the most restrictive assumptions we have made thus far is the deterministic regularity of the re-exposure in both dose magnitude and inter-exposure interval. Many factors we do not include in our model are likely to drive a stochastic pattern of re-exposure to an infection circulating in a community (e.g., strain mutation (Ferguson

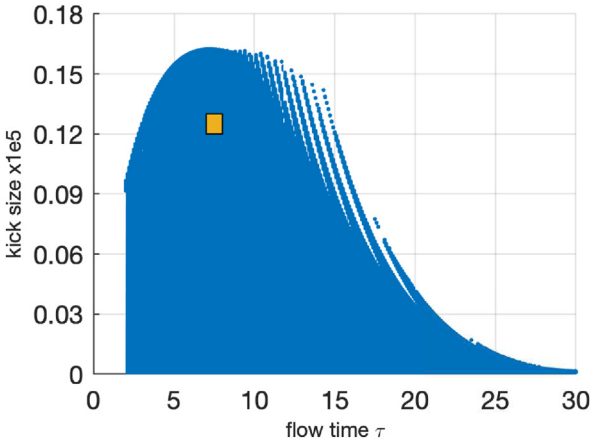

Fig. 5. The periodic viral re-exposure dose required to provide long-term protection against reinfection depends on the inter-exposure interval. The blue area corresponds to parameter values (τ, k) for which the deterministic flow-kick system has a stable flow-kick equilibrium, i.e. the combination of inter-exposure interval and dose magnitude provides long-term protection against reinfection. The small yellow box depicts the set $7 < \tau < 8$ and $12000 < k < 13000$ from which the viral re-exposure dose and inter-exposure period are randomly sampled (uniformly) in the stochastic simulation in Fig. 6.

et al., 2003), seasonality in transmissibilty of the pathogen (James et al., 2012), birth rates impacting frequency of outbreaks among naive susceptibles (Conlan & Grenfell, 2007), etc. (James et al., 2012; Lofgren et al., 2007)). To explore the impact of stochasticity in our model system, we selected a region of the parameter space that would be expected to be fully protected against reinfection under an assumption of deterministic regularity (see the yellow block region in Fig. 5). We then sampled randomly (uniformly) from within that region to provide a stochastic pattern of re-exposure dose magnitudes and inter-exposure intervals.

By disrupting the regularity of the re-exposure pattern in this way, we see a very different immune response, in which many of the stochastic re-exposure patterns lead to reinfection (see Fig. 6). We emphasize that the re-exposure parameters were all sampled from within the yellow box in Fig. 5, and therefore would not lead to reinfection in a deterministic scenario. The stochastic nature of the re-exposure appears to be reducing the successful protection in host immune response by perturbing the system away from the region of the deterministic flow-kick equilibria. Work is already underway to discover what properties of this seemingly simple mathematical system lead to this counter-intuitive outcome, including the use of techniques from the literature on Piecewise Deterministic Markov Processes.

4. Discussion

Mathematical modeling of epidemics is usually considered on a population scale but, in fact, epidemics emerge from individuals catching infections and infecting others. While some recent models have investigated the immune-

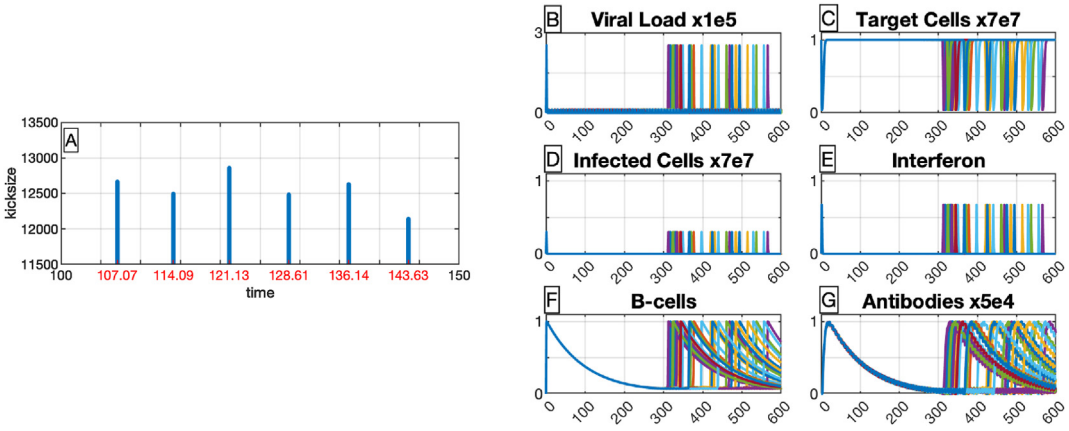

Fig. 6. Stochastic simulation of the flow-kick system. **(A)** An example of stochastic kicks and viral exposures sampled uniformly from the set $7 < \tau < 8$, $12000 < k < 13000$ depicted in Fig. 5. **(B)**–**(G)** A subset of stochastic simulations are plotted here. Out of 500 simulations, 386 (77%) had an excursion representing reinfection by $t = 600$.

epidemiological coupling of individuals to populations (e.g. (Kostova, 2007; Xue & Xiao, 2020),), they have primarily focused on how within-host replication eventually spills over to between-host transmission. Our model builds on, and complements, these studies. It focuses on the within-host dynamics of an individual during an ongoing epidemic outbreak. We assume individuals experience frequent sub-infective "boosting" exposures due to the epidemic. The within-host dynamics in this model are meant to capture symptomatic infection, rather than asymptomatic or carrier states of infection.

Our model demonstrates how ongoing individual immune function may be "primed" by sub-infectious doses. The possibility of priming suggests that low, endemic circulation of clinically infectious cases might need to be characterized by both the traditional reproductive number, R_0 and also by an analogous Priming value, P_{eff}. The priming value measures the number of cases prevented by boosting the undetected, ongoing protection that exists in a non-naïve population. Current estimates of R_{eff} (Andrade & Duggan, 2022) would include some of these posited protective effects when estimated from real-world data. However, those estimates would not include the important distinction between long-term and actively reinforced short-term immune protection in the recovered population. This has potential to affect our understanding not only of the epidemiological dynamics themselves, but also related aspects of disease ecology and evolution (e.g., the evolution of virulence for pathogens over time (Bull & Lauring, 2014)).

Untangling the effects of R_0 and P_{eff} allows us to make rigorous and quantitative predictions. For example, standard theory would conflate the following cases: (1) a population that has experienced a large-scale outbreak in which everyone has residual protective, long-lasting adaptive immune memory; (2) a population in which symptomatic cases in an ongoing outbreak become limited due to "boosting" effects caused by sustained re-exposures to subclinical doses. The latter would be possible when there is an ongoing, low-level endemic prevalence of active infectious cases. For these two scenarios, our model allows us to anticipate differences in how the populations would react to subsequent reintroduction of infection. Specifically, actual eradication of the infection from circulation would leave the latter population susceptible to a severe outbreak from re-introduction of the infection. The loss of long-term immune protection can be estimated by fitting ongoing incidence curves for observed reinfection to the initial epidemic. In the presence of boosting, this estimated loss will be slower than the actual loss-rate for adaptive immune memory.

While our model has very strong structural assumptions, and we have purposefully investigated only short-term immune dynamics within a single host, the insights it provides have implications for longer-term dynamics. One implication is that endemic prevalence would have a more important role in whether or not large breakthrough outbreaks occur than is usually assumed. This is due to the non-trivial relationship between prevalence and the frequency of re-exposures. Our model shows that, depending on frequency, these re-exposures lead either to "boosting" or active reinfection.

In this model, we considered only a single pathogen with a single circulating strain. Our results exploring stochastic kicks within an otherwise "safe" region, in which regular re-exposure would continue to provide protection, hint at potentially complex dynamics. It is possible that the maintenance of stable short-term protection against reinfection depends on the specific dynamics of the innate and adaptive immune responses. The co-circulation of multiple pathogens that prime the upregulation of innate immune responses in similar ways, but do not have cross-protective adaptive immune responses, may meaningfully de-couple these dynamics. This means that a full pathogen-level ecosystem analysis may be needed to truly understand and predict the presence of boosting. In this way, our work also parallels and complements the rich existing literature considering the conditions under which exogenous re-exposure to pathogen can lead to successive outbreaks at the population level (Singh & Myers, 2014), especially in cases such as zoonotic spillover due to host contact with heterospecfic animal reservoirs (Lloyd-Smith et al., 2009; Roche et al., 2012). Fully understanding how both endogenous and exogenous re-exposure, at both the within- and among-host levels, can together shape outbreak dynamics remains an open and challenging area for further exploration. Moreover, pathogens provide an evolutionary selective landscape for each other's circulation (Fefferman et al., 2022; Haeryfar, 2020; Hanna et al., 2015). Perhaps they also shape the severity (e.g., observable R_0 and virulence) of each other's outbreaks through perturbing host innate and adaptive immune function by altering the timing of upregulation (even when they do not offer cross-protective adaptive immunity). This is a potential area for further study.

The model presented in this paper only begins to scratch the surface of the work needed to truly understand these dynamics. We used numerical solutions of a single parameterization of a single model. We have not yet explored alternative functional forms for system elements, nor considered extending the model to capture longer-term immune dynamics (either in addition, or as an alternative, to short-term immune function). We have not analyzed the boundary between periodic exposure patterns that give stable protection and those that trigger eventual reinfection, and we have not explained the counter-intuitive result that stochastic exposure patterns reduce the protection conveyed by regular exposure patterns. Clearly, the eventual understanding of which elements are driving the complex behavior of the system is a tantalizing goal. We hope that this first presentation will attract more interest from the field and highlight the value of using flow-kick systems as a simplifying abstraction for multiscale coupling of within-host and among-host dynamics in epidemic outbreaks.

Declaration of competing interest

The authors declare that they have no known competing financial interests or personal relationships that could have appeared to influence the work reported in this paper.

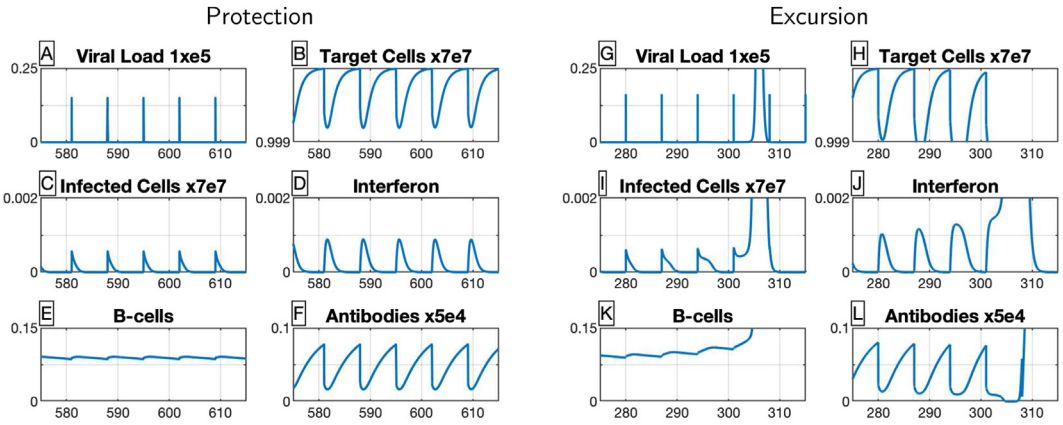

Fig. A1. **(A)**–**(F)** A flow-kick equilibrium corresponding to Fig. 4 A-F, with $\tau = 7$, $k = 15000$. This is an example of protection against deterministically periodic repeated re-exposure. **(G)**–**(L)** The dynamics close to excursion in a flow-kick system with $\tau = 7$, $k = 16244$. This corresponds to Fig. 4 G-L.

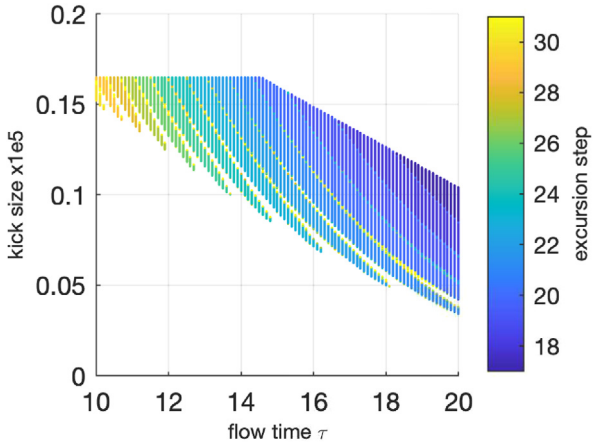

Fig. A2. This figure colors the complement of Fig. 5. For each (τ, k), the color indicates the iteration number of the deterministic flow-kick system associated with the first re-infection. The white region on the lower left is associated with locations that never show reinfection, corresponding to the blue protection region in Fig. 5. There is banding in the iteration number, starting at iteration number 17 on the upper right and going to iteration number 30 on the upper left. Regions associated with constant iteration numbers are separated by regions associated with canard-like behavior.

Acknowledgements

This work was supported in part by the Mathematics and Climate Research Network and AIM through NSF award DMS-1722578, and the Clare Boothe Luce Program through Boston University, with additional support from Bowdoin College. We are grateful to the anonymous reviewers for productive feedback, and special thanks to Timothy Chumley for helpful discussions during the revision process.

References

Alexander, F., Huang, W., & Agusto, F. (2022). Exploring the effects of prescribed fire on tick spread and propagation in a spatial setting. *Computational and Mathematical Methods in Medicine*, 2022.
Allen, L. J. S., Brown, V. L., Jonsson, C. B., Klein, S. L., Laverty, S. M., Magwedere, K., Owen, J. C., & Van Den Driessche, P. (2012). Mathematical modeling of viral zoonoses in wildlife. *Natural Resource Modeling, 25*(1), 5–51.
Anderson, R. M., & May, R. M. (1992). *Infectious diseases of humans: Dynamics and control*. Oxford university press.
Andrade, J., & Duggan, J. (2022). Inferring the effective reproductive number from deterministic and semi-deterministic compartmental models using incidence and mobility data. *PLoS Computational Biology, 18*(6), Article e1010206.
Beutler, B. (2004). Innate immunity: An overview. *Molecular Immunology, 40*(12), 845–859.
Bonilla, F. A., & Oettgen, H. C. (2010). Adaptive immunity. *Journal of Allergy and Clinical Immunology, 125*(2), S33–S40.
Brauer, F., Van den Driessche, P., Wu, J., & Allen, L. J. S. (2008). *Mathematical epidemiology* (Vol. 1945). Springer.
Brodin, P., & Davis, M. M. (2017). Human immune system variation. *Nature Reviews Immunology, 17*(1), 21–29.
Brooke, R. J., Kretzschmar, M. E. E., Mutters, N. T., & Teunis, P. F. (2013). Human dose response relation for airborne exposure to coxiella burnetii. *BMC Infectious Diseases, 13*(1), 1–8.
Buchanan, R. L., Smith, J. L., & Long, W. (2000). Microbial risk assessment: Dose-response relations and risk characterization. *International Journal of Food Microbiology, 58*(3), 159–172.
Bull, J. J., & Lauring, A. S. (2014). Theory and empiricism in virulence evolution. *PLoS Pathogens, 10*(10), Article e1004387.

Cao, P., Yan, A. W. C., Heffernan, J. M., Petrie, S., Moss, R. G., Carolan, L. A., Guarnaccia, T. A., Kelso, A., Barr, I. G., McVernon, J., Laurie, K. L., & McCaw, J. M. (2015). Innate immunity and the inter-exposure interval determine the dynamics of secondary influenza virus infection and explain observed viral hierarchies. *PLoS Computational Biology, 11*(8), Article e1004334.
Castillo-Chavez, C., Blower, S., Van den Driessche, P., Kirschner, D., & Yakubu, A.-A. (2002). *Mathematical approaches for emerging and reemerging infectious diseases: Models, methods, and theory* (Vol. 126). Springer Science & Business Media.
Chou, T., & D'Orsogna, M. R. (2022). A mathematical model of reward-mediated learning in drug addiction. *Chaos: An Interdisciplinary Journal of Nonlinear Science, 32*(2), Article 021102.
Conlan, A. J. K., & Grenfell, B. T. (2007). Seasonality and the persistence and invasion of measles. *Proceedings of the Royal Society B: Biological Sciences, 274*(1614), 1133–1141.
Cope, R. C., Ross, J. V., Chilver, M., Stocks, N. P., & Mitchell, L. (2018). Characterising seasonal influenza epidemiology using primary care surveillance data. *PLoS Computational Biology, 14*(8), Article e1006377.
Fefferman, N. H., Price, C. A., & Stringham, O. C. (2022). Considering humans as habitat reveals evidence of successional disease ecology among human pathogens. *PLoS Biology, 20*(9), Article e3001770.
Ferguson, N. M., Galvani, A. P., & Bush, R. M. (2003). Ecological and immunological determinants of influenza evolution. *Nature, 422*(6930), 428–433.
Gale, P. (2001). Developments in microbiological risk assessment for drinking water. *Journal of Applied Microbiology, 91*(2), 191–205.
Gale, P. (2005). Land application of treated sewage sludge: Quantifying pathogen risks from consumption of crops. *Journal of Applied Microbiology, 98*(2), 380–396.
Glass, K., & Grenfell, B. T. (2004). Waning immunity and subclinical measles infections in england. *Vaccine, 22*(29–30), 4110–4116.
Gunn, J. S., Marshall, J. M., Baker, S., Dongol, S., Charles, R. C., & Ryan, E. T. (2014). Salmonella chronic carriage: Epidemiology, diagnosis, and gallbladder persistence. *Trends in Microbiology, 22*(11), 648–655.
Haeryfar, S. M. M. (2020). On invariant t cells and measles: A theory of "innate immune amnesia". *PLoS Pathogens, 16*(12), Article e1009071.
Hanna, S., Barrès, B., Vale, P. F., & Laine, A.-L. (2015). Co-infection alters population dynamics of infectious disease. *Nature Communications, 6*(1), 1–8.
Hart, W. S., Hochfilzer, L. F. R., Cunniffe, N. J., Lee, H., Nishiura, H., & Thompson, R. N. (2019). Accurate forecasts of the effectiveness of interventions against ebola may require models that account for variations in symptoms during infection. *Epidemics, 29*, Article 100371.
Hock, K., & Fefferman, N. H. (2012). Social organization patterns can lower disease risk without associated disease avoidance or immunity. *Ecological Complexity, 12*, 34–42.
Hoyer-Leitzel, A., & Iams, S. (2021). Impulsive fire disturbance in a savanna model: Tree–grass coexistence states, multiple stable system states, and resilience. *Bulletin of Mathematical Biology, 83*(11), 1–25.
James, T., Fraser, C., Simon, C., Meeyai, A., Hinsley, W., Donnelly, C. A., Ghani, A., & Ferguson, N. (2012). Essential epidemiological mechanisms underpinning the transmission dynamics of seasonal influenza. *Journal of The Royal Society Interface, 9*(67), 304–312.
Keeling, M. J., & Rohani, P. (2011). *Modeling infectious diseases in humans and animals*. Princeton University Press.
Keeling, M. J., & Td Eames, K. (2005). Networks and epidemic models. *Journal of the royal society interface, 2*(4), 295–307.
Kostova, T. (2007). Persistence of viral infections on the population level explained by an immunoepidemiological model. *Mathematical Biosciences, 206*(2), 309–319.
Kretzschmar, M., & Wallinga, J. (2009). Mathematical models in infectious disease epidemiology. In *Modern infectious disease epidemiology* (pp. 209–221). Springer.
Lavine, J. S., King, A. A., Andreasen, V., & Bjørnstad, O. N. (2013). Immune boosting explains regime-shifts in prevaccine-era pertussis dynamics. *PLoS One, 8*(8), Article e72086.
Lloyd-Smith, J. O., George, D., Pepin, K. M., Pitzer, V. E., Pulliam, J. R. C., Dobson, A. P., Hudson, P. J., & Grenfell, B. T. (2009). Epidemic dynamics at the human-animal interface. *Science, 326*(5958), 1362–1367.
Lloyd-Smith, J. O., Schreiber, S. J., Kopp, P. E., & Getz, W. M. (2005). Superspreading and the effect of individual variation on disease emergence. *Nature, 438*(7066), 355–359.
Lofgren, E., Fefferman, N. H., Naumov, Y. N., Gorski, J., & Naumova, E. N. (2007). Influenza seasonality: Underlying causes and modeling theories. *Journal of Virology, 81*(11), 5429–5436.
Lofgren, E. T., Halloran, M. E., Rivers, C. M., Drake, J. M., Porco, T. C., Lewis, B., Yang, W., Vespignani, A., Shaman, J., Eisenberg, J. N. S., Eisenberg, M. C., Marathe, M., Scarpino, S. V., Alexander, K. A., Meza, R., Ferrari, M. J., Hyman, J. M., Meyers, L. A., & Stephen, E. (2014). Mathematical models: A key tool for outbreak response. *Proceedings of the National Academy of Sciences, 111*(51), 18095–18096.
Maul, A. (2014). Heterogeneity: A major factor influencing microbial exposure and risk assessment. *Risk Analysis, 34*(9), 1606–1617.
Meyer, K., Hoyer-Leitzel, A., Iams, S., Klasky, I., Lee, V., Stephen, L., Bussmann, E., & Lou Zeeman, M. (2018). Quantifying resilience to recurrent ecosystem disturbances using flow–kick dynamics. *Nature Sustainability, 1*(11), 671–678.
NM Kraay, A., Hayashi, M. A. L., Hernandez-Ceron, N., Spicknall, I. H., Eisenberg, M. C., Meza, R., & Eisenberg, J. N. S. (2018). Fomite-mediated transmission as a sufficient pathway: A comparative analysis across three viral pathogens. *BMC Infectious Diseases, 18*(1), 1–13.
Pascucci, E., & Pugliese, A. (2021). Modelling immune memory development. *Bulletin of Mathematical Biology, 83*(12), 1–22.
Peter Parham. (2014). *The immune system*. Garland Science.
Roche, B., Dobson, A. P., Guégan, J.-F., & Rohani, P. (2012). Linking community and disease ecology: The impact of biodiversity on pathogen transmission. *Philosophical Transactions of the Royal Society B: Biological Sciences, 367*(1604), 2807–2813.
Saad-Roy, C. M., Jessica, C., Metcalf, E., & Grenfell, B. T. (2022). Immuno-epidemiology and the predictability of viral evolution. *Science, 376*(6598), 1161–1162.
Saad-Roy, C. M., Wingreen, N. S., Levin, S. A., & Grenfell, B. T. (2020). Dynamics in a simple evolutionary-epidemiological model for the evolution of an initial asymptomatic infection stage. *Proceedings of the National Academy of Sciences, 117*(21), 11541–11550.
Silk, M. J., & Fefferman, N. H. (2021). The role of social structure and dynamics in the maintenance of endemic disease. *Behavioral Ecology and Sociobiology, 75*(8), 1–16.
Singh, S., & Myers, C. R. (2014). Outbreak statistics and scaling laws for externally driven epidemics. *Physical Review E, 89*(4), Article 042108.
Stephen, I., Vincent, N., & Noonburg, E. G. (2016). Alternative stable states, coral reefs, and smooth dynamics with a kick. *Bulletin of Mathematical Biology, 78*(3), 413–435.
Tamen, A. T., Dumont, Y., Tewa, J. J., Bowong, S., & Couteron, P. (2016). Tree–grass interaction dynamics and pulsed fires: Mathematical and numerical studies. *Applied Mathematical Modelling, 40*(11–12), 6165–6197.
Tamen, A. T., Dumont, Y., Tewa, J.-J., Bowong, S., & Couteron, P. (2017). A minimalistic model of tree–grass interactions using impulsive differential equations and non-linear feedback functions of grass biomass onto fire-induced tree mortality. *Mathematics and Computers in Simulation, 133*, 265–297.
Teunis, P. F. M., Moe, C. L., Liu, P., Miller, S. E., Lindesmith, L., Baric, R. S., Le Pendu, J., & Calderon, R. L. (2008). Norwalk virus: How infectious is it? *Journal of Medical Virology, 80*(8), 1468–1476.
Villa, E., Fattovich, G., Mauro, A., & Pasino, M. (2011). Natural history of chronic hbv infection: Special emphasis on the prognostic implications of the inactive carrier state versus chronic hepatitis. *Digestive and Liver Disease, 43*(S8–S14).
Xue, Y., & Xiao, Y. (2020). Analysis of a multiscale hiv-1 model coupling within-host viral dynamics and between-host transmission dynamics. *Mathematical Biosciences and Engineering, 17*(6), 6720–6736.
Zeeman, M. L., Meyer, K., Bussmann, E., Hoyer-Leitzel, A., Iams, S., Klasky, I. J., … Stephen, L. (2018). Resilience of socially valued properties of natural systems to repeated disturbance: A framework to support value-laden management decisions. *Natural Resource Modeling, 31*(3), Article e12170.